NASA Technical Memorandum 106034

Dynamic Analysis of Free-Piston Stirling Engine/Linear Alternator-Load System-Experimentally Validated

M. David Kankam
National Aeronautics and Space Administration
Lewis Research Center
Cleveland, Ohio

Jeffrey S. Rauch
Sverdrup Technology, Inc.
Lewis Research Center Group
Brook Park, Ohio

and

Walter Santiago
National Aeronautics and Space Administration
Lewis Research Center
Cleveland, Ohio

Prepared for the
27th Intersociety Energy Conversion Engineering Conference
cosponsored by the ANS, SAE, ASC, AIAA, IEEE, and AIChE
San Diego, California, August 3–7, 1992

NASA

"Dynamic Analysis of Free-Piston Stirling Engine/Linear Alternator-Load System - Experimentally Validated"

M. David Kankam
NASA Lewis Research Center
Cleveland, Ohio

Jeffrey S. Rauch
Sverdrup Technology, Inc.
Lewis Research Center
Brook Park, Ohio

Walter Santiago
NASA Lewis Research Center
Cleveland, Ohio

ABSTRACT

This paper discusses the effects of variations in system parameters on the dynamic behavior of a Free-Piston Stirling Engine/Linear Alternator (FPSE/LA)-load system. The mathematical formulations incorporate both the mechanical and thermodynamic properties of the FPSE, as well as the electrical equations of the connected load. State-space technique in the frequency domain is applied to the resulting system of equations to facilitate the evaluation of parametric impacts on the system dynamic stability. Also included is a discussion on the system transient stability as affected by sudden changes in some key operating conditions.

Some representative results are correlated with experimental data to verify the model and analytic formulation accuracies. Guidelines are given for ranges of the system parameters which will ensure an overall stable operation.

INTRODUCTION

The free-piston Stirling engine/linear alternator (FPSE/LA) is an attractive, thermoelectric energy conversion system for space applications due to its potential for long life and reliability. However, when integrated into a power system with connected load(s), system performance must be evaluated to ensure that unfavorable system interactions do not occur. Treatment of such interactions is not commonly found in the existing literature which deals mainly with establishing the engine operating conditions (Refs.1 to 7). Additionally, a combination of detailed representations of the engine thermodynamics and nonlinearities, and load modeling has not received widespread attention.

This paper describes a general dynamic analysis of a FPSE/LA connected to a load. The objective of the paper is two-fold. First, the paper demonstrates the application of the state-space technique (Ref. 8) to model the dynamics of a FPSE/LA-load system. This technique is then used to predict the impact of some key system parameters and operating conditions on the dynamic stability of a Space Power Research Engine (SPRE)/LA-load system at NASA Lewis Research Center (Ref. 9).

The mathematical model used for the FPSE is based on the recommendations in Ref. 10. The analysis incorporates the engine dynamics and thermodynamics, and detailed modeling of the LA and connected load(s). The state-space formulation used in the analysis is a modern control theory approach of representing a system by its state variables. By definition, a minimum set of n state variables, typically denoted by "X", is necessary for a complete description of the internal status or state of the system. The state-space designates the n-variable co-ordinate space in which X ranges. The representation of the system equations by the compact state-space model (SSM) permits the application of powerful vector-matrix theory, and can readily be relegated to a computer to yield a complete description of the system.

The simulation, performed on the MATLAB software (Ref. 11), yields results in the form of root locus plots of the system eigenvalues (Ref. 8). The plots show the migration of the system roots caused by parametric variations and, hence, the effects of such variations on the stability margins of the SPRE/LA-load system. The advantage of the frequency-domain-based eigenvalue analysis is its single computation of the exact modes of oscillation of the dynamic system. Also, it can complement, valuably, information obtained by time-domain simulation and testing of a physical system. Many practical systems are nonlinear. However, the usefulness of the linearized eigenvalue analysis is its use in identifying potential worst-case operating conditions which can then be verified by nonlinear time-domain analysis and, possibly, testing. Hence, by using the appropriate input data, the analytic method and results such as reported in this paper can be used to expedite, or assist in, the development of requirements for the application of a FPSE/LA in a space power system.

STUDY SYSTEM

The analytic formulations discussed in this paper relate to a system which consists of a single cylinder FPSE connected to an LA via the engine power piston. Figure 1 depicts a block diagram representation of the study system. The LA output terminals in series with a tuning capacitor, C_T, feed through a load controller to an external load. The controller may be used to "dump" excess generated electric power, in the case where power demand (by the external load) is less than the power supplied by the engine/alternator source. In this case, the load controller acts to maintain power balance. When the load demand exceeds the generated power, the engine will tend to stall.

ANALYTIC APPROACH

The overall performance equations of the FPSE/LA-load system are developed in three stages. First, the equations describing the dynamics of the FPSE are derived. This is followed by the subsystem comprising the LA, parasitic load and an external load. Finally, the combined system equation is formulated for subsequent analysis.

DYNAMIC EQUATIONS OF FPSE

The following simplifying assumptions are made - (1) Schmidt's thermodynamic analysis is evoked such that:

(a) the displacer and piston motions and the working space pressure are sinusoidal

(b) the working fluid obeys the ideal gas law, and expands and compresses isothermally

(2) The working space gas pressure is constant but time-variant.

(3) The bounce space pressure balances the average working space pressure. Hence, average positions of the power piston, displacer and cylinder casing are stationary.

The dynamic equations of the FPSE/LA system, incorporating the mechanical and thermodynamic properties of the Stirling engine, is stated in EQ (1).

$$[M_M][\ddot{X}] + [C_M + C_T][\dot{X}] + [K_M + K_T][X] = [F_E] \tag{1}$$

where the mechanical system matrices are:

$$[M_M] = \text{displacer (D) and pistion (P) mass matrix} = \begin{bmatrix} m_D & O \\ O & m_p \end{bmatrix}$$

and m_D and m_p are the displacer and piston masses, respectively;

$$[C_M] = \text{damping matrix} = \begin{bmatrix} C_{DD} & C_{DP} \\ C_{PD} & C_{PP} \end{bmatrix}$$

and

$$[K_M] = \text{stiffness matrix} = \begin{bmatrix} K_{DD} & K_{DP} \\ K_{PD} & K_{PP} \end{bmatrix}$$

The element C_{DD} is the total damping coefficient of the displacer; that is, the sum of the displacer -to -engine casing (or ground), C_D, and the displacer-piston coupling C_{PD}. Similarly, the total piston damping C_{PP} comprises the self term C_P and piston-displacer coupling C_{DP}. These definitions also apply to the stiffness matrix, $[K_M]$. The external force vector $[F_E]$ consists of the displacer and piston components F_{ED} and F_{EP}, respectively. Typically, F_{ED} is nonexistent.

The matrices $[C_T]$ and $[K_T]$ are associated with the engine thermodynamic force vector $[F_T]$ expressed in EQ 2. The negative sign denotes the restoring nature of the force $[F_T]$.

$$[F_T] = -\{[C_T][\dot{X}] + [K_T][X]\} \tag{2}$$

The details of derivations of the engine equations are documented in Ref. 12. The force $[F_T]$ is expressed in EQ (3), where A_D, A_R and A_p are the displacer, displacer rod and piston areas, respectively. The parameter P_c is the compression space pressure on the displacer and piston. The term P_{HX} is the heat exchanger pressure difference between the expansion pressure P_E and P_c. The displacer and piston components of $[F_T]$ are F_{TD} and F_{TP}, respectively.

$$[F_T] = \begin{bmatrix} F_{TD} \\ F_{TP} \end{bmatrix} = \begin{bmatrix} +A_D & -A_R \\ O & -A_p \end{bmatrix} \begin{bmatrix} P_{HX} \\ P_C \end{bmatrix} = [A_T]\,[P_T] \tag{3}$$

The thermodynamic pressure P_T is assumed a linearly dependent function mainly of position and velocity. Hence, EQ (3) may be recast into EQ (4), where the superscript P denotes partial derivatives of the pressure terms in EQ (5).

$$[F_T] = [A_T]\,[P_T] = [A_T]\,\{[C^P][\dot{X}] + [K^P][X]\} \tag{4}$$

$$[C^P] = \begin{bmatrix} \dfrac{\delta P_{HX}}{\delta \dot{X}_D} & \dfrac{\delta P_{HX}}{\delta \dot{X}_P} \\ \dfrac{\delta P_C}{\delta \dot{X}_D} & \dfrac{\delta P_C}{\delta \dot{X}_P} \end{bmatrix}$$

$$[K^P] = \begin{bmatrix} \dfrac{\delta P_{HX}}{\delta X_D} & \dfrac{\delta P_{HX}}{\delta X_P} \\ \dfrac{\delta P_C}{\delta X_D} & \dfrac{\delta P_C}{\delta X_P} \end{bmatrix} \tag{5}$$

Comparison of EQS (2) and (4) implies the relationship of EQ (6).

$$\begin{aligned} [C_T] &= -[A_T][C^P] \\ [K_T] &= -[A_T][K^P] \end{aligned} \tag{6}$$

Equation (5) requires that each of P_{HX} and P_C must be a continuous function of the piston position and velocity.

EVALUATION OF $[K^P]$ AND $[C^P]$

The matrices $[K^P]$ and $[C^P]$ and, hence, $[K_T]$ and $[C_T]$ may be obtained from Schmidt's thermodynamic analysis. However, this leads to an optimistic prediction of engine performance, since Schmidts's analysis neglects the thermodynamic and fluid frictional losses. Better estimates of the $[K^P]$ and $[C^P]$ matrices may be evaluated from a more inclusive analysis inherent in the GLIMPS (Refs. 13 and 14) and HFAST (Ref. 15) design codes, or test data.

The pressure terms P_c and P_{HX} are obtainable from the design codes, for given piston and displacer positions and speeds. For any Stirling engine, the partials in EQ (5) are constant with respect to the engine dynamics and, thus, can be frozen in analytic computations. Additional simplifying assumptions are that the partials $\frac{\partial P_c}{\partial X_D}$, $\frac{\partial P_c}{\partial X_P}$, $\frac{\partial P_{HX}}{\partial X_D}$ and $\frac{\partial P_{HX}}{\partial X_P}$ are all negligible. Substitution of the reduced EQ (5) into EQ (4) results in EQ (7), in

$$\begin{bmatrix} P_{HX} \\ P_C \end{bmatrix} = \begin{bmatrix} \frac{\partial P_{HX}}{\partial X_D} & \frac{\partial P_{HX}}{\partial X_P} \\ 0 & 0 \end{bmatrix} \begin{bmatrix} \dot{X}_D \\ \dot{X}_P \end{bmatrix} + \begin{bmatrix} 0 & 0 \\ \frac{\partial P_C}{\partial X_D} & \frac{\partial P_C}{\partial X_P} \end{bmatrix} \begin{bmatrix} X_D \\ X_P \end{bmatrix} \tag{7}$$

which the pressure, position and speed terms are complex, and can be obtained from the aforementioned design codes or test. Equation (7) yields a total of four real and imaginary equations from which the real-only partials are solved. Subsequently, EQS (8) are obtained from EQ (6) and the resulting EQ (5). The expanded dynamic EQ (9) results from EQS (1) and (8).

$$\left.\begin{aligned} [C_H] &= \begin{bmatrix} C_{H11} & C_{H12} \\ C_{H21} & C_{H22} \end{bmatrix} = \begin{bmatrix} -A_D \frac{\partial P_{HX}}{\partial X_D} & -A_D \frac{\partial P_{HX}}{\partial X_P} \\ 0 & 0 \end{bmatrix} \\ [K_H] &= \begin{bmatrix} K_{H11} & K_{H12} \\ K_{H21} & K_{H22} \end{bmatrix} = \begin{bmatrix} A_P \frac{\partial P_C}{\partial X_D} & A_P \frac{\partial P_C}{\partial X_P} \\ A_P \frac{\partial P_C}{\partial X_D} & A_P \frac{\partial P_C}{\partial X_P} \end{bmatrix} \end{aligned}\right\} \tag{8}$$

$$\left.\begin{aligned} &\begin{bmatrix} M_D & 0 \\ 0 & M_P \end{bmatrix} \begin{bmatrix} \ddot{X}_D \\ \ddot{X}_P \end{bmatrix} = -\begin{bmatrix} C_{11} & C_{12} \\ C_{21} & C_{22} \end{bmatrix} \begin{bmatrix} \dot{X}_D \\ \dot{X}_P \end{bmatrix} - \begin{bmatrix} K_{11} & K_{12} \\ K_{21} & K_{22} \end{bmatrix} \begin{bmatrix} X_D \\ X_P \end{bmatrix} + \begin{bmatrix} 0 \\ F_{EP} \end{bmatrix} \\ &\textit{where} \\ &\begin{bmatrix} C_{11} & C_{12} \\ C_{21} & C_{22} \end{bmatrix} = \begin{bmatrix} (C_{DD} + C_{T11}) & (C_{DP} + C_{T12}) \\ (C_{PD} + C_{T21}) & (C_{PP} + C_{T22}) \end{bmatrix} \\ &\begin{bmatrix} K_{11} & K_{12} \\ K_{21} & K_{22} \end{bmatrix} = \begin{bmatrix} (K_{DD} + K_{T11}) & (K_{DP} + K_{T12}) \\ (K_{PD} + K_{T21}) & (K_{PP} + K_{T22}) \end{bmatrix} \end{aligned}\right\} \tag{9}$$

Thermoelectric power generation requires connection of the FPSE to an electromechanical device, such as a linear alternator and an associated load. Modelling of the alternator-load system is discussed next.

ELECTRICAL EQUATIONS OF LA-LOAD MODEL

An equivalent circuit diagram of the LA is shown in Fig. 3. The alternator output terminals are connected through a series tuning capacitor C_T to a parallel combination of a parasitic load R_p and an external series R_L - L_L - C_L static load. The capacitor C_T serves to ensure an electrical resonance within the circuit and, hence, a maximum power transfer from the engine-alternator system to the connected load. The stability of the system may be enhanced by ensuring a coincidence or near coincidence of the electrical resonant and the mechanical operating frequencies. The other parameters in the figure are the stator resistance, R_g, the leakage inductance, L_g, the magnetizing inductance, L_m, and the eddy current and hysteresis loss term R_c in the magnetic core of the LA.

Application of Kirchhoff's voltage law to loops 1 through 3 yields EQS (10) to (12) in which the term $\dot{f}$ denotes $\frac{df}{dt}$ and,

$$(R_g + R_p) i_g - R_p i_L + (L_g + L_m)\dot{i}_g - L_m \dot{i}_1 + V_{C_T} = e_g \tag{10}$$

$$R_c i_1 - L_m \dot{i}_g + L_m \dot{i}_1 = 0 \tag{11}$$

$$-R_p i_g + (R_p + R_L) i_L + L_L \dot{i}_L + V_{C_T} = 0 \tag{12}$$

in terms of the engine piston-induced flux change, the generated alternator voltage is:

$$e_g = -\left(N \frac{d\Phi}{dX_p}\right) \dot{X}_p \tag{13}$$

The capacitor voltages are stated in EQS (14) and (15).

$$\dot{V}_{C_T} = i_g/C_T \tag{14}$$

$$\dot{V}_{C_L} = i_L/C_L \tag{15}$$

The term Φ is the flux linking the N turns of the LA magnetic material. Solution of EQS (10) to (13) results in the derivative currents summarized in EQS (16) to (18).

$$\dot{I}_g = \left[-(R_e + R_p)i_g - R_c i_1 + R_p i_L - V_{C_T} - \left(N\frac{d\Phi}{dx_p}\right)\dot{x}_p\right]\Big/ L_e \tag{16}$$

$$\dot{i}_1 = \left[-(R_e + R_p)i_g + R_p i_L - V_{C_T} - \left(N\frac{d\Phi}{dx_p}\right)\dot{x}_p\right]\Big/ L_e - R_c\left(\frac{1}{L_e} + \frac{1}{L_m}\right)i_1 \tag{17}$$

$$\dot{i}_L = (R_p i_g - (R_p + R_L)i_L - V_{C_L})/L_L \tag{18}$$

STATE-SPACE REPRESENTATION

The external force F_{EP} (EQ (9)) on the piston is represented by the term $\left(N\frac{d\Phi}{dt}\right)|_g$. The system state variable vector is defined in EQ (19),

$$[X]^T = [x_D\ \dot{x}_D\ x_p\ \dot{x}_p\ i_g\ i_1\ i_L\ V_{C_T}\ V_{C_L}] = [X_1\ X_2\ X_3\ X_4\ X_5\ X_6\ X_7\ X_8\ X_9] \tag{19}$$

where the superscript "T" denotes transposition of the vector.

Substitution of the state variable EQ (19) into the FPSE dynamic equations (9), and into the LA-load equations (14) to (18) yields the state-space model of EQ (20),

$$\left.\begin{aligned}[\dot{X}] &= [A][X] + [B][U]\\ [Y] &= [C][X] + [D][U]\end{aligned}\right\} \tag{20}$$

The elements of the 9×9 [A]-matrix of EQ (21) are defined earlier. The selected state variables are all physically measurable and can, therefore, constitute the system outputs [Y]. Thus, [Y] is 9×1 vector and the control matrix [C] equals a 9×9 identity matrix [I]. If the engine oscillation is initiated by a unity step input to the piston, with subsequent motion of the displacer, then the input vector $[U]^T = [U_D U_P] = [0\ \ 1]$. Hence, [D] is a 9×2 null matrix.

The matrix [A] contains all the individual and coupled variables of the study system. The damping and stiffness coefficients contain the engine nonlinear contributions. However, the matrices [A], [B], [C] and [D] are all numerically constant. Such a linear time-invariant (LTI) system can be subjected to small perturbation analysis about an operating point, to determine the overall system dynamic behavior.

Evaluation of the eigenvalues of the [A]-matrix requires knowledge of all its elements. The only available set of complete data pertains to the SPRE/LA system connected to an R-L load. The static load is parasitic and mainly resistive with small but finite inductance. There is no separate external load as such. Furthermore, the existing data shows no core loss resistance for the alternator model. Imposition of these simplifications on Fig. 3 results in the state variable vector and system matrix as defined in EQS (22) and (23), where the subscript S denotes simplified electrical model. These equations are used in the analysis of the SPRE/LA-load system.

$$[A] = \begin{vmatrix} 1 & & & & & & & & \\ -K_{11}/m_D & -C_{11}/m_D & -K_{12}/m_D & -C_{12}/m_D & & & & & \\ & & 1 & & & & & & \\ -K_{21}/m_p & -C_{21}/m_p & -K_{22}/m_p & -C_{22}/m_p & \left(\frac{Nd\Phi}{dx_p}\right)/m_p & & & & \\ & & & -\left(\frac{Nd\Phi}{dx_p}\right)/L_e & -(R_e + R_p)/L_e & R_p/L_e & -R_p/L_e & -1/L_e & \\ & & & & R_p/L_L & -(R_p + R_L)/L_L & & & -1/L_L \\ & & & -\left(\frac{Nd\Phi}{dx_p}\right)/L_e & -(R_e + R_p)/L_e & R_p/L_e & -R_c\left(\frac{1}{L_e} + \frac{1}{L_m}\right) & -1/L_e & \\ & & & & 1/C_T & & & & \\ & & & & & 1/C_L & & & \end{vmatrix} \tag{21}$$

$$[X]_s^T = [X_D \dot{X}_D X_P \dot{X}_P i_g V_{C_T}] = [X_1 X_2 X_3 X_4 X_5 X_6] \quad (22)$$

$$[A]_s = \begin{bmatrix} 0 & 1 & 0 & 0 & 0 & 0 \\ -K_{11}/m_D & -C_{11}/m_D & -K_{12}/m_D & -C_{12}/m_D & 0 & 0 \\ 0 & 0 & 0 & 1 & 0 & 0 \\ -K_{21}/m_P & -C_{21}/m_P & -K_{22}/m_P & -C_{22}/m_P & (N\frac{\partial \Phi}{\partial x_P})/m_P & 0 \\ 0 & 0 & 0 & \frac{-(N\frac{\partial \Phi}{\partial x_P})}{(L_e+L_{ac}+L_L)} & \frac{-(R_e+R_L)}{(L_e+L_{ac}+L_L)} & \frac{-1}{(L_e+L_{ac}+L_L)} \\ 0 & 0 & 0 & 0 & 1/c_T & 0 \end{bmatrix} \quad (23)$$

METHOD OF ANALYSIS

The SSM of the coupled equations are simulated using the MATLAB software. Variations are enforced in key system and operating parameters to induce a migration of the system eigenvalues in the frequency plane. The effect of a parameter on the eigenvalues is determined by varying only that parameter about its nominal or design value, while keeping all other parameters at their nominal values. A plot of the eigenvalue movement due to changes in a given parameter yields the corresponding root locus.

Dynamic analysis derives its strength from its ability to predict the time-domain behavior of an LTI system via simple calculations in the frequency domain. This is exemplified by Fig. 4 (Ref. 16) which shows time histories for corresponding eigenvalues in the frequency domain. The upper part of the plot is typically mirrored in the lower half. Exponentially increasing oscillations are evident for the eigenvalue in the right-hand plane. This dynamic instability, in the case of a FPSE, will be equivalent to a piston overstroke. An eigenvalue on the jw-axis is critically stable, since the oscillation amplitudes are constant. This is characteristic of, and desired for a FPSE as an oscillator. An eigenvalue in the left-hand plane is dynamically stable. However, a FPSE in this mode of operation is described as stalling or falling out, since the oscillations decay with time.

The foregoing discussions are used to characterize the simulation results.

DISCUSSION OF RESULTS

The interactions between the FPSE/LA subsystem and the connected load are illustrated Figs. 5 to 12. The nominal and/or design values of the parameters used in the simulation are summarized in Table 1 which represents the "base" or reference system. All the values shown are measured quantities. However, zero values are enforced for the partials of the heat exchanger pressure with respect to the piston and displacer velocities. The difficulty associated with measurement of these partials casts doubt on the accuracy of their values. Unless otherwise indicated, selected parameters are varied from 50 to 150 percent of their nominal value, in increments of 25 percent. The arrows connecting the "X's" in the plots signify the directions of the eigenvalue movements, due to parametric changes.

BASE SYSTEM - Figure 5 shows a set of eigenvalues for the coupled FPSE/LA-load system, and another set for the decoupled FPSE and LA-load subsystems. The electrical and mechanical roots for the coupled base system are identified as E, and MP and MD, respectively. The terms MP and MD refer to the piston and displacer eigenvalues, respectively. The terms EU, and MPU and MDU denote the electrical and mechanical roots for the uncoupled FPSE and LA-load subsystems. The uncoupling is realized by setting the A (5,4) and A (4,5) elements to zero in EQ (23) of the simplified electrical model.

In the case of the uncoupled subsystems, the computed 98.6 Hz of the electrical root compares nearly exactly with hand-calculated 98.3 Hz from the characteristic equation of the electrical subsystem. The average of the predicted piston and displacer frequencies is 107.1 Hz. This is only 2 percent and 5.8 percent above the design and operating frequencies 105 and 101.1 Hz, respectively, of the SPRE. It is noteworthy that the piston root MPU in the right-hand plane (RHP) is characteristic of an oscillator with exponentially increasing amplitudes towards its mechanical limits. This is consistent with Redlich and Berchowitz's observation (Ref. 2).

The coupled system shows a slight increase in the average engine frequency, namely, 111 Hz. Again, this is within 10 percent of either the design or operating frequency of the SPRE. Also, the coupled engine tends

to reduce the margin of stability of the electrical system. However, the effect of the LA-load subsystem is to push the MPU root to the MP position, nearly on the jw-axis. Hence, the electrical system acts as an external means of control, and forces the engine to perform as an oscillator. The engine is said to be critically stable in that it oscillates with constant amplitudes. Finally, the unequal piston and displacer frequencies indicate that in the practical engine, the piston stored energy/energy dissipated in a cycle is not necessarily the same as that of the displacer.

The following discussions will highlight the influence of various parameters on the coupled system roots E, MP and MD and, hence, the system dynamic stability.

LA Resistance (R_a) - Varying the alternator resistance from 50 to 150 percent of its nominal value has insignificant effect on the system roots which remain almost stationary in Fig. 6. The relatively small value of the nominal resistance of 0.082Ω may account for its ineffectiveness.

LA Leakage Inductance (L_a) - A definite effect on the system roots caused by varying L_a is evident in Fig. 7. The symbols "X" of the base system are identified by self-directed arrows from MD, MP and E. Increasing L_a from 50 percent of nominal can place the piston root MP on the jw-axis, while improving the damping of the electrical root E. The displacer root gets pushed towards the jw-axis, but remains in the LHP. Further increase in L_a beyond the nominal value may destabilize the engine, unless this is prevented by some external feedback control system. Thus, the nominal L_a is considered near optimum for the piston root.

Tuning Capacitance (C_T) - Figure 8 shows that a 50 to 150 percent variation of the nominal tuning capacitance has an effect similar to that caused by the leakage inductance. Here, the optimum capacitance for placing the piston root on the jw-axis is between 100 and 112 percent of the nominal value.

Load Resistance (R_L) - The pronounced impact of the load resistance variation from 50 to 300 percent of its nominal value is illustrated in Fig. 9. Increasing R_L significantly improves the electrical damping, with only a modest change in its frequency. The piston root can not only be moved past the jw-axis, but also, its frequency decreases gradually. Initially, the frequency of the displacer root reduces only slightly, while its damping increases. Beyond 150 percent of the nominal R_L, the damping reduces with further increase in R_L. Examination of Fig. 9 shows that, as R_L increases further, the piston root is pulled into the RHP, while the displacer root moves towards the jw-axis. These counter-balancing effects will tend to stabilize the engine. Since it is the larger of the two resistances in the system, the load resistance can mask the influence of the LA resistance.

The above observation shows that, generally, a properly designed parasitic load may be used to force the FPSE/LA subsystem to operate as an oscillator; that is, one eigenvalue pair on the jw-axis, and all others in the LHP.

Short Circuit Condition - A potentially hazardous operating condition in a FPSE/LA-load system is a short circuit of the load. This represents an extreme case of load impedance variation. Figure 10 depicts the positions of the system roots for such a condition. The electrical root nearly collapses on the jw-axis, without substantial change in frequency, when compared to the base system. With only the small alternator resistance remaining in the electrical circuit, the shorted electrical circuit approximates an oscillator. The piston root is forced into the RHP, signifying exponentially increasing oscillations. Hence, the effect of a sudden short circuit condition is to render the engine unstable, with a possible consequence of piston overstroke. In the physical system, this situation may result from generated energy which is dissipated in a minimum impedance of the electrical system.

Open Circuit Condition - Another possible but undesirable operating scenario is an open circuit condition. This, also, is an extreme form of load inpedance variation. The electrical roots in Fig. 11 collapse onto the origin, with their damping capability eliminated. The engine becomes unstable, as the piston roots are in the RHP. This condition is also possible in a practical system in which the generated energy, in the form of power, abruptly has no path to flow.

CONCLUSIONS

This paper uses the state-space technique to determine the effects of parametric variations on the dynamic stability of a FPSE/LA-load system. The mathematical formulation includes the major thermodynamic effects of the engine. The following conclusions are based on the evaluation of stability of the SPRE/LA-load system. However, the analytical approach and trends of the results are applicable to other FPSE/LA-load systems.

The results confirm Redlick and Berchowitz's classical control theory-based result that there exists only one mode of oscillation for the FPSE. This mode is denoted by a pair of mechanical roots in the right side of the complex plane. Such roots must be forced by a control mechanism to move onto the jw-axis, to ensure the engine behaviour as a constant amplitude oscillator.

For a given FPSE/LA subsystem, the operating frequency can be load dependent. However, the effect of the constituent load components depends on the their relative magnitudes. A system-designed load generally aids in stabilizing the system. Dynamic stability is reasonably assured, if the electrical system parameters do not change significantly from their design values. For the system studied, the parameters with the most impact

on the system stability are the LA leakage inductance, the tuning capacitance and the load resistance.

Abnormal operating conditions, such as a sudden short or open circuit of the load, can destabilize the engine, unless ameliorating controls are in place.

Generally, the effects of parametric variations on the system dynamic stability give an insight into the engine-alternator-load interactions. This information can be valuable during design stage, and with respect to performance prediction to guide system evaluation in experimental work.

REFERENCES

1. Rauch, J.S., "Steady-state Analysis of Free-Piston Stirling Engine Dynamics," IECEC '75 Record, pp. 961-965.
2. Redlich, R.N., Berchowitz, D.M., "Linear Dynamics of Free-Piston Stirling Engines," Proc. Instr. Mech. Engrs., Vol. 199, #A3, pp. 203-213, 1985.
3. Das, R.L. Bahrami, K.A., "Dynamics and Control of Stirling Engines in a 15 KWe Solar Electric Generation Concept," Proc. IECEC 1979, pp. 133–138.
4. Benvenuto, G., DeMonte, F., Farina, F., "Dynamic Behavior Prediction of Free-Piston Stirling Engines," IECEC 1990, pp. 346-351.
5. Cichy, M. Carlini, M., "Frequency Dynamic Analysis of Free-Piston Stirling Engines," IECEC 1984, pp. 1829-1835.
6. Carlini, M. Kucharski, T., "Dynamic Analysis of Free-Piston Stirling Engines by Modal Transformation Method," Presented at SAE Intl. Congress and Exposition, Detroit, MI, Feb. 24-28, 1986.
7. Chen, N.C.J., Griffin, F.P., "Linear Harmonic Analysis of Free-Piston Stirling Engines," ORNL/CON-172, Martin Marietta Energy Systems, Inc., Oak Ridge Natl. Lab., June 1986.
8. "Modern Control Theory", Book, by W.L. Brogan, Prentice-Hall Inc., 1982.
9. "Space Power Demonstrator Engine", Phase I Final Report, NASA Contractor Report 179555, May 1987.
10. Kankam, M.D., Rauch, J.S., "Comparative Survey of Dynamic Analyses of Free-Piston Stirling Engines," IECEC, August 1991, Boston/NASA TM-104491, 1991.
11. "MAC II MATLAB," Copyright The Mathwork, 1987, 1988.
12. Rauch, J.S., Kankam, M.D., "Free-Piston Stirling Engine Dynamics," NASA TM, 1992.
13. Gedeon, D., "A Globally - Implicit Stirlig Cycle Simulation," 21st IECEC, Vol. 1, 1986, American Chemical Society, pp. 550-556.
14. Gedeon, D., "GLIMPS Version 4.0 User's Manual," 1992, by Gedeon Associates.
15. Huang, S.C., "HFAST-A Harmonic Analysis Program for Stirling Cycles," 27th IECEC, Aug. 1992, San Diego.
16. "Subsynchronous Resonance," Seminar Notes, General Electric Company, 1979.

Figure 1. - Block diagram representation of study system.

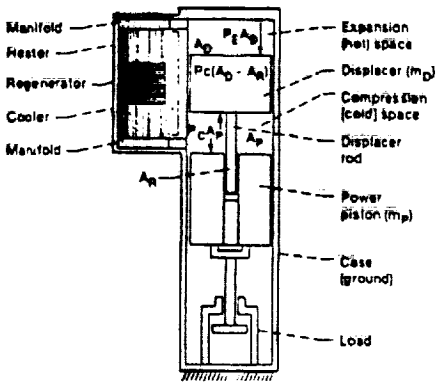

Fig. 2 Schematic of a single cylinder Free-Piston Stirling Engine

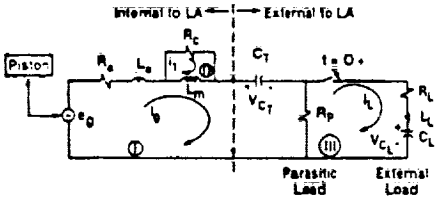

Figure 3. - Equivalent circuit of linear alternator (LA)-load system.

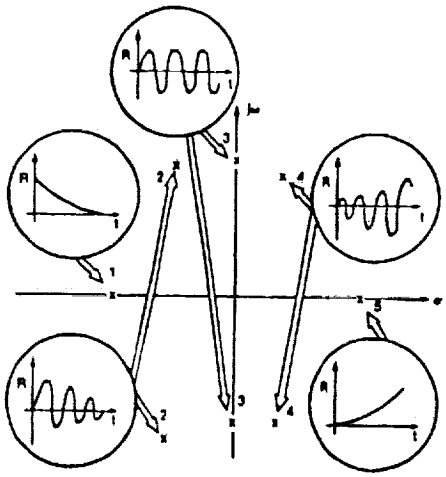

Fig. 4 Illustrating modal responses of eigenvalues

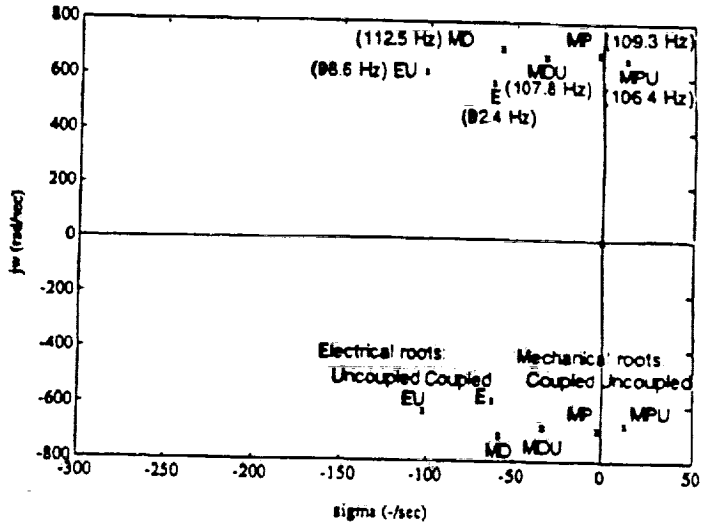

Fig. 5 Plot of coupled and decoupled system eigenvalues

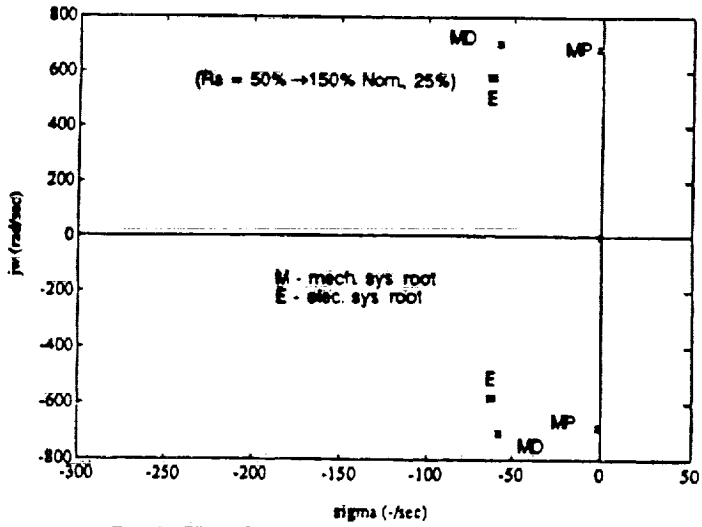

Fig. 6 Plot of system eigenvalues with Ra variation

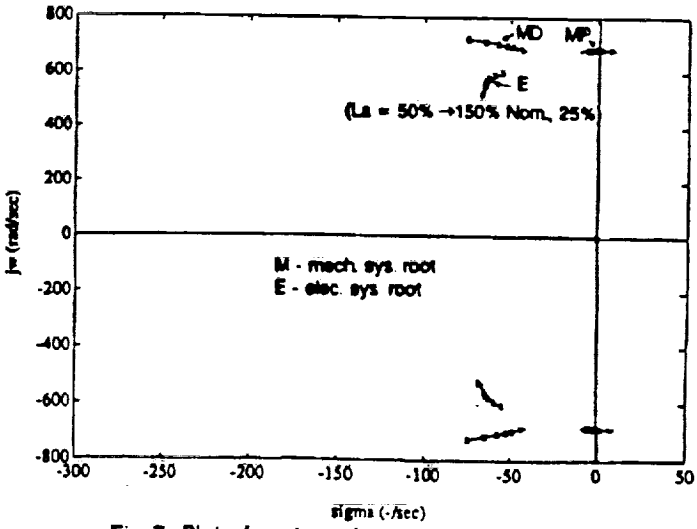

Fig. 7 Plot of system eigenvalues with La variation

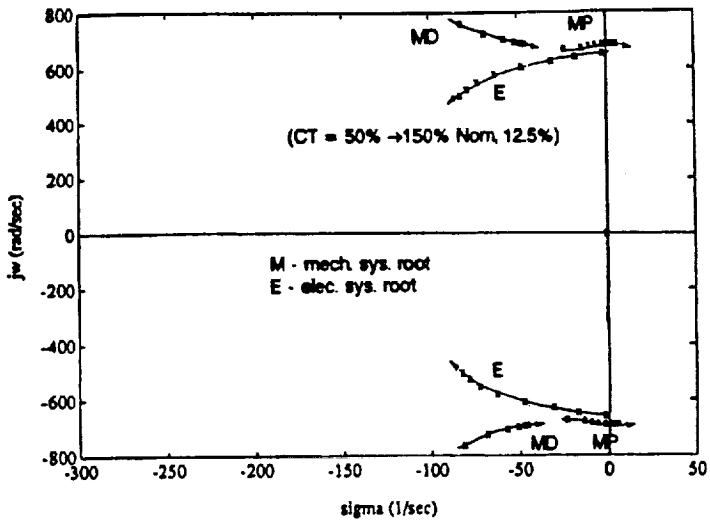

Fig. 8 Plot of system eigenvalues with CT variation

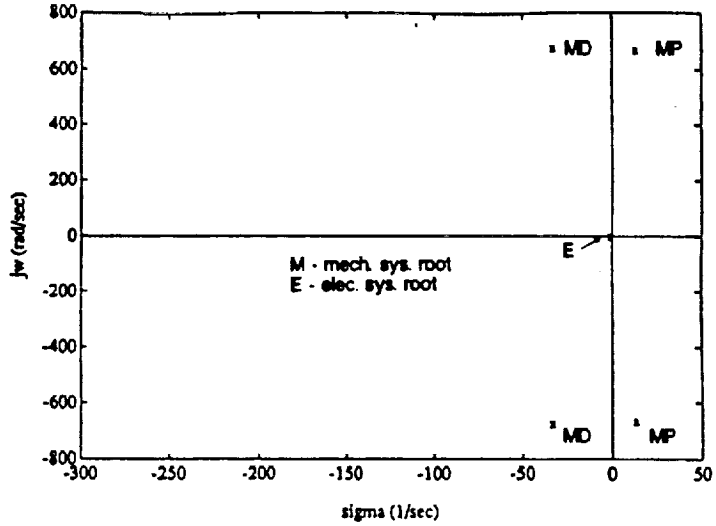

Fig. 11 Plot of system eigenvalues with open circuit

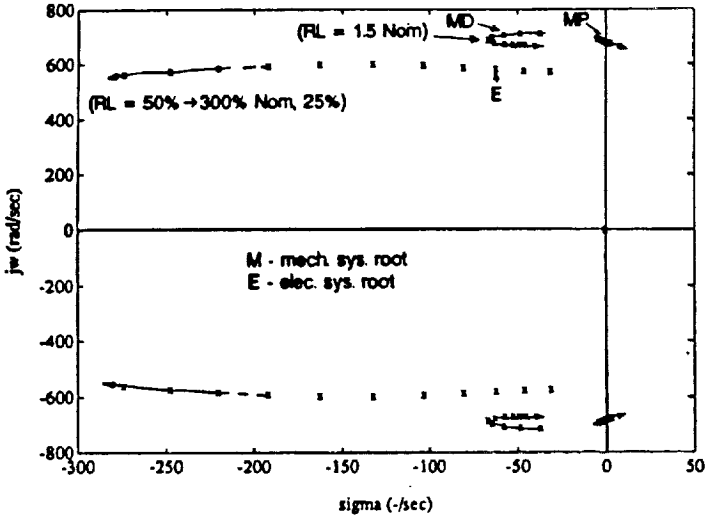

Fig. 9 Plot of system eigenvalues with RL variation

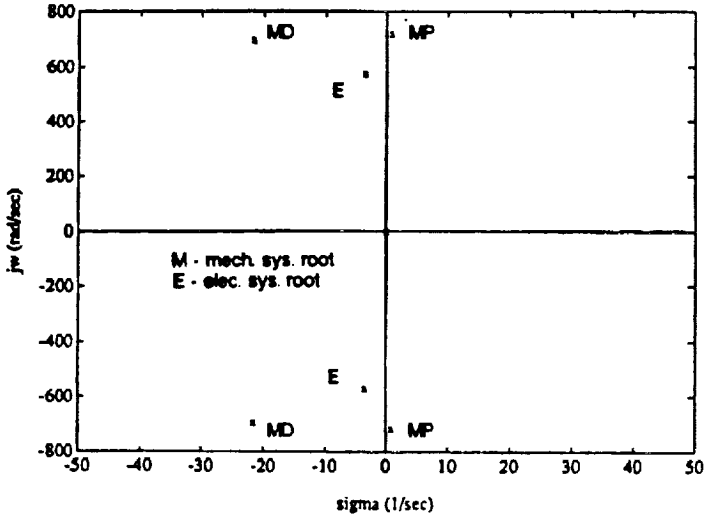

Fig. 10 Plot of system eigenvalues with short circuit

Table 1 Summary of System Parameters

Symbol	Value	Description
m_d	1.701 (kg)	Displacer mass
m_p	9.968 (kg)	Piston mass
A_p	164.63 x 10^{-4} (m^2)	Piston area
A_d	102.61 x 10^{-4} (m^2)	Displacer area
A_{rp}	2.887 x 10^{-4} (m^2)	Piston rod area
K_d	0.1197 x 10^5 (N/m)	Displacer total stiffness coefficient
C_d	54.95 (N.S/m)	Displacer total damping coefficient
K_p	12.205 x 10^5 (N/m)	Piston total stiffness coefficient
C_p	60.85 (N.S/m)	Piston total damping coefficient
K_{dp}	0 (N/m)	Displacer-piston coupling stiffness coefficient
K_{pd}	0 (N/m)	Piston-displacer coupling stiffness coefficient
C_{dp}	0 (N.S/m)	Displacer-piston coupling damping coefficient
C_{pd}	0 (N.S/m)	Piston-displacer coupling damping coefficient
$\frac{\partial P_c}{\partial x_p}$	186.562 x 10^5 (N/m^3)	Compression space pressure change with piston position
$\frac{\partial P_c}{\partial x_d}$	-24.98 x 10^5 (N/m^3)	Compression space pressure change with displacer position
$\frac{\partial P_c}{\partial \dot{x}_p}$	0 ($N.S/m^3$)	Compression space pressure change with piston velocity
$\frac{\partial P_c}{\partial \dot{x}_d}$	0 ($N.S/m^3$)	Compression space pressure change with displacer velocity
$\frac{\partial P_{hx}}{\partial x_p}$	0 (N/m^3)	Heat exchanger pressure change with piston position
$\frac{\partial P_{hx}}{\partial x_d}$	0 (N/m^3)	Heat exchanger pressure change with displacer position
$\frac{\partial P_{hx}}{\partial \dot{x}_d}$	0 ($N.S/m^3$)	Heat exchanger pressure change with displacer velocity
$\frac{\partial P_{hx}}{\partial \dot{x}_p}$	0 ($N.S/m^3$)	Heat exchanger pressure change with piston velocity
$N\frac{\partial \Phi}{\partial x_p}$	45.5 (V·S/m)	Magnetic flux linkage change with piston position
R_{LA}	0.082 (Ω)	LA winding resistance
L_{LA}	1.95 (mH)	LA leakage inductance
L_m	6.50 (mH)	LA magnetizing inductance
C_t	296.3 (μF)	Tuning capacitance
R_L	1.6655 (Ω)	Load resistance
L_L	0.121 (mH)	Load inductance

REPORT DOCUMENTATION PAGE

Form Approved
OMB No. 0704-0188

1. AGENCY USE ONLY (*Leave blank*)	2. REPORT DATE	3. REPORT TYPE AND DATES COVERED
	August 1992	Technical Memorandum

4. TITLE AND SUBTITLE

Dynamic Analysis of Free-Piston Stirling Engine/Linear Alternator-Load System-Experimentally Validated

5. FUNDING NUMBERS

WU-590-13-11

6. AUTHOR(S)

M. David Kankam, Jeffrey S. Rauch, and Walter Santiago

7. PERFORMING ORGANIZATION NAME(S) AND ADDRESS(ES)

National Aeronautics and Space Administration
Lewis Research Center
Cleveland, Ohio 44135-3191

8. PERFORMING ORGANIZATION REPORT NUMBER

E-7017

9. SPONSORING/MONITORING AGENCY NAMES(S) AND ADDRESS(ES)

National Aeronautics and Space Administration
Washington, D.C. 20546-0001

10. SPONSORING/MONITORING AGENCY REPORT NUMBER

NASA TM- 106034

11. SUPPLEMENTARY NOTES

Prepared for the 27th Intersociety Energy Conversion Engineering Conference cosponsored by the ANS, SAE, ASC, AIAA, IEEE, and AIChE, San Diego, California, August 3-7, 1992. M. David Kankam, NASA Lewis Research Center, Cleveland, Ohio; Jeffrey S. Rauch, Sverdrup Technology, Inc., Lewis Research Center Group, 2001 Aerospace Parkway, Ohio 44142; and Walter Santiago, NASA Lewis Research Center, Cleveland, Ohio. Responsible person, M. David Kankam, (216) 433-6143.

12a. DISTRIBUTION/AVAILABILITY STATEMENT

Unclassified - Unlimited
Subject Category 66

12b. DISTRIBUTION CODE

13. ABSTRACT (*Maximum 200 words*)

This paper discusses the effects of variations in system parameters on the dynamic behavior of the Free-Piston Stirling Engine/Linear Alternator (FPSE/LA)-load system. The mathematical formulations incorporate both the mechanical and thermodynamic properties of the FPSE, as well as the electrical equations of the connected load. State-space technique in the frequency domain is applied to the resulting system of equations to facilitate the evaluation of parametric impacts on the system dynamic stability. Also included is a discussion on the system transient stability as affected by sudden changes in some key operating conditions. Some representative results are correlated with experimental data to verify the model and analytic formulation accuracies. Guidelines are given for ranges of the system parameters which will ensure an overall stable operation.

14. SUBJECT TERMS

Free-piston Stirling engine/LA-load; Dynamic stability; System analysis; Mathematical models; State-space technique

15. NUMBER OF PAGES

10

16. PRICE CODE

A02

17. SECURITY CLASSIFICATION OF REPORT	18. SECURITY CLASSIFICATION OF THIS PAGE	19. SECURITY CLASSIFICATION OF ABSTRACT	20. LIMITATION OF ABSTRACT
Unclassified	Unclassified	Unclassified	